Surface Science 640 (2015) 25–35

Contents lists available at ScienceDirect

Surface Science

journal homepage: www.elsevier.com/locate/susc

Cutting a chemical bond with demon's scissors: Mode- and bond-selective reactivity of methane on metal surfaces

A. Lozano [a], X.J. Shen [b,c], R. Moiraghi [a], W. Dong [b], H.F. Busnengo [a,*]

[a] Grupo de Fisicoquimica en Interfases y Nanoestructuras, Instituto de Fsica Rosario, CONICET and Universidad Nacional de Rosario, Bv. 27 de Febrero 210 bis, 2000 Rosario, Argentina
[b] Laboratoire de Chimie, UMR 5182 CNRS, Ecole Normale Supérieure de Lyon, Site Jacques Monod, 46, Allée d'Italie, 69364 Lyon Cedex 07, France
[c] State Key Laboratory of Molecular Reaction Dynamics and Center for Theoretical Computational Chemistry, Dalian Institute of Chemical Physics, Chinese Academy of Science, 116023 Dalian, People's Republic of China

ARTICLE INFO

Available online 9 April 2015

Keywords:
Methane
Surfaces
Molecular dynamics
Adsorption
Reactive force fields
Bond selectivity

ABSTRACT

In this paper we discuss several aspects of methane reactive sticking on Pt(111) in the light of supersonic molecular beam experiments (including state-resolved measurements) and quasi-classical trajectory calculations based on an accurate reaction specific reactive force field constructed from Density Functional Theory (DFT) data. With the aim of understanding the origin of the full bond selectivity recently achieved experimentally and to predict how selectivity depends on the collision conditions, we discuss in detail, the role of initial translational and (mode-specific) vibrational energy of CH_4 and all its deuterated isotopomers, as well as surface temperature effects. Last but not least, the systematic and detailed theoretical analysis presented here serves as an illustration of the possibilities and usefulness of accurate reaction specific reactive force fields built from DFT data. This approach allows investigating dynamical aspects of the interaction of polyatomic molecules on surfaces through quasi-classical trajectory calculations accounting for the full dimensionality of the system (including both molecular and surface degrees of freedom): something that a few years ago was just a dream for the gas–surface dynamics community.

1. Introduction

James Clerk Maxwell, the great Scottish physicist, conceived an imaginary creature capable of realizing some processes unlikely to happen in reality, e.g., turning a cup of well mixed milk tea into two layers with the milk on top and the tea at bottom. Such an imaginary creature is now named as Maxwell demon and usually used by physicists to describe some thought experiments. Chemists resort seldom to such a demon to describe whatever processes in chemical reactions. Nevertheless, we will show that the bond-selective reactivity in the dissociative adsorption of methane isotopomers on some metal surfaces looks quite like the action of a Maxwell demon.

The dissociative adsorption of light hydrocarbons on transition-metal surfaces is a key step in various technologically important processes, e.g., catalytic steam reforming, and growth of graphene by chemical vapor deposition [1–5]. A large number of experimental results are now available for methane dissociation on Ni and Pt surfaces and this makes such systems the benchmarks for reactions of polyatomic molecules on metal surfaces. Reactive scattering experiments using supersonic molecular beams with resolved initial states have revealed unambiguously mode- and bond-selective reactivity of methane on Ni and Pt surfaces [6–10]. Many chemical reactions can take place only when an activation energy is provided, e.g., the cleavage of one C–H bond in a methane molecule upon its collision with a Pt(111) surface requiring at least ~ 0.8 eV. The very characteristic feature of the mode-selective reactivity is that the activation efficiency depends not only on the amount of energy but also on the way in which it is imparted to the molecule. It was shown experimentally that the energy deposited into a vibrational mode (in particular, a stretching mode) is more efficient for dissociating a methane molecule on Ni(111) than depositing the same amount into the translational degree of freedom (DOF) of the center of mass of the molecule [6,8]. Furthermore, Beck et al. [7] have shown that a roughly equal amount of energy deposited into two vibrational modes, one stretching a single C–H bond of CH_2D_2 and the other stretching both of them, results in a higher dissociation probability of the molecule on Ni(100) for the former.

All the partially deuterated isotopomers of methane have the same electronic structure. Thus, the activation energy is the same for cleaving a C–H or a C–D bond. Therefore, from the point of view based purely on energetics, achieving a selective scission of one of the two types of bonds seems to be possible only for Maxwell demon. Nevertheless, the different masses of H and D atoms result in different stretching modes for C–H and C–D bonds. By exciting precisely a mode stretching a C–H bond with a laser, the groups of Utz and Beck have succeeded in achieving the full selective cleavage of a C–H bond of some deuterated methane isotopomers upon its collision with Ni(111) [10] or Pt(111) surfaces [11], respectively.

* Corresponding author.
E-mail address: busnengo@ifir-conicet.gov.ar (H.F. Busnengo).

http://dx.doi.org/10.1016/j.susc.2015.04.002
0039-6028/

Before the experiments revealing the mode- and bond-selective reactivity of methane on Ni and Pt surfaces, there were two competing theoretical models, based on very different assumptions, to account for the methane dissociative adsorption on metal surfaces. One is a statistical model based on the assumption that the adsorbate–surface collision complex allows for very fast energy redistribution between different DOFs [12–14]. Due to the fast randomization of energies associated with different DOFs, only the total amount of energy of the molecule matters and the statistical model does not predict any mode- or bond-selective reactivity. The inadequacy of such an assumption has been revealed unambiguously by the experimental finding of mode- and bond-selective reactivity of methane on Ni and Pt surfaces.

Another model relies on the dynamical description of reacting systems. As surface reactions are concerned, the dissociative adsorption of a diatomic molecule on a solid surface has been studied most extensively with the hydrogen dissociation on various metal surfaces as one prototypical reaction [15–19]. The two basic ingredients of a dynamic model are 1) a potential energy surface (PES) and 2) a method for describing the dynamics of the reacting system. The degree of difficulty for studying a given system is determined by the complexity and some key characteristics of its PES, e.g., dimensionality, landscape, barrier height, etc. Within the approximation of a rigid substrate, the PES for the dissociation of a diatomic molecule on a solid surface is a six-dimensional (6D) one. Now, various methods exist for constructing reliable 6D PES for the dissociative adsorption of diatomic molecules on solid surfaces (see e.g., Refs. [20] and [21] as well as references therein). However, many successful methods for constructing PES of diatomic molecules, in particular those based on interpolation, can be hardly extended to deal with PES of higher dimensionality. Therefore, building a reliable PES which accounts for all the DOFs of methane and also those of the surface atoms on an equal footing is already a theoretical challenge.

Early investigations on the dissociation dynamics of methane on metal surfaces have been carried out with quantum dynamics methods. Such methods are computationally very demanding and the state-of-the-art ones can only afford an explicit description of about a dozen of DOFs. For quantum dynamics investigations, it is necessary to simplify the description of the system in order to reduce the DOFs to be considered explicitly. Some early studies have been made with a drastically simplified model, i.e., quasi-diatomic model which treats the methyl group as a single entity [22–26]. The quasi-diatomic model has some obvious drawbacks. First, the vibration spectrum of such a model has nothing to do with the true spectrum of methane. Hence, this excludes any attempt to study mode-selective reactivity. Since there is only one cleavable bond in this model, it is also out of the question to study bond-selective reactivity. To alleviate the severe limitations of the quasi-diatomic model, Jackson and Nave have proposed a more elaborate model, called reaction path Hamiltonian (RPH) [27,28]. In this model, the stretching of one C–H bond along the minimum energy path is fully described while all the other DOFs perpendicular to the reaction coordinate are modeled by a harmonic approximation. The improvement provided by this model with respect to the quasi-diatomic model is that it gives the correct vibration spectrum of an isolated methane molecule within the harmonic approximation and thus allows for investigating the mode-selective reactivity. It is worthwhile to note that the reaction path Hamiltonian inherits also some characters of the quasi-diatomic model. Since only the stretching of one C–H bond is fully described and the stretching of the other three C–H bonds is described with a parabolic potential which does not allow for bond breaking, the RPH is a model with only one cleavable C–H bond like the quasi-diatomic model and thus prevents studying the bond-selective reactivity.

Recently, Guo's group has constructed a 12D PES for CH_4/Ni(111) in order to carry out a quantum dynamics study [29]. The strategy for reducing the number of DOFs was applied directly in the dynamics calculation by imposing the C_{3v} symmetry to the methyl group. Because of this symmetry constraint, the three C–H bonds of the constrained methyl group are stretched or compressed simultaneously. In principle, these three bonds can be broken at the same time but such a simultaneous cleavage of three C–H bonds costs much energy and does not take place without the supply of a huge amount of energy. The imposed C_{3v} symmetry modifies the vibration spectrum of the molecule with in principle all the modes being affected except the totally symmetric one. This renders impossible the study of mode-selective reactivity for some modes, i.e., those most affected by the symmetry constraint. Moreover, imposing the C_{3v} symmetry predestines the cleavable C–H bond and thus excludes the possibility to study bond-selective reactivity. Both the RPH proposed by Jackson and Nave and the model studied by Guo's group can be qualified as models with one-active C–H bond. To the best of our knowledge, quantum dynamics calculations have been performed only for such models with only one-active C–H bond until now. It is to note also that in the quantum dynamics studies reported so far, the translational DOFs of methane parallel to the surface were not considered explicitly (to reduce the total number of DOFs) and dynamics calculations were performed only for the incidence of the molecule at a top site. The effect of the impact points at the surface was accounted for by an ad hoc post-treatment [26,27,29,28].

Experiments showed that surface temperature has a significant effect on the sticking probability of methane on metal surfaces, in particular for the molecule at low incident energies [30–32]. Accounting for the surface temperature the effect from first principles requires explicit consideration of the DOFs of surface atoms in dynamics calculations. This is far beyond of the capability of any state-of-the-art quantum dynamics method and appears out of reach of such methods even in the foreseeable future. In all the previous quantum dynamics studies, the surface temperature effect has been treated with some ad hoc approximations [27].

Once an approach for determining the interatomic forces is prescribed, quasi-classical molecular dynamics (QCMD) simulations can be carried out also for studying surface reaction dynamics. In the case that a pre-constructed PES is available, the straightforward calculation of interatomic forces allows fast molecular dynamics (MD) simulations to be performed within the framework of quasi-classic method. As already pointed out above, some of the established interpolation methods to construct a PES for diatomic molecules interacting with surfaces [33], cannot be easily extended to consider polyatomic molecules or the surface degrees of freedom. Reactive force fields (RFFs) provide an alternative approach capable of dealing with, in principle, much more DOFs. For the dissociative adsorption of hydrogen on Pd(111), we have shown that a carefully parameterized RFF allows for describing adequately the effect of surface temperature by dealing with the DOFs of the substrate on an equal footing of the adsorbate DOFs [34,35]. Recently, we have also demonstrated the feasibility of constructing accurate PES by using RFFs for methane dissociation on Ni and Pt surfaces [36]. These RFFs render now possible full-dimensional MD simulations of the dissociative adsorption of methane on Ni(111) and Pt(111) surfaces, including even the DOFs of the substrate.

QCMD simulations can be performed also with an ab initio molecular dynamics (AIMD) method in which the interatomic forces are calculated on the fly from highly time-consuming electronic-structure calculations. AIMD has been applied by Groß and co-workers to study hydrogen dissociative adsorption on Pd surfaces [37,38]. But, for the dissociation of methane on a metal surface, AIMD simulation becomes much more complicated since the dissociation probability is lower by several orders of magnitude than that for hydrogen dissociation on a transition metal surface and a huge number of trajectories are needed to obtain statistically meaningful results ($\sim 10^6$ in the region of low incident energies). Nevertheless, Nattino et al have reported recently some results for CHD_3/Pt(111) of AIMD calculations performed in the region of high incident energies where the dissociation probability is relatively high [39].

In this feature article, we will summarize the key characteristics of the reactive force fields we developed for describing methane dissociative adsorption on a metal surface. We show also how our approach allows for addressing an important issue unexplored theoretically until recently, i.e., simulating bond-selective reactivity and predicting new possible

conditions for bond selectivity. Finally, some perspectives opened by our approach for future theoretical investigations will be pointed out.

2. Reactive force fields

2.1. Background

First, we make a brief review about the development of reactive force fields which is, by no means, exhaustive and we refer only to those works most closely connected to what we present here. The most popular reactive force fields used nowadays [40] are rooted in an original work by Rose et al. [41,42] who showed the existence of a universal relation between binding energy variation and bond distortions. Inspired by these results, Abell [43] derived a single formula adequate for both metallic and covalent bonding systems. The important underlying concept is the variation of the binding energy with the bond order between atoms in different chemical environments. Later, Tersoff [44] proposed an analytical functional form to build a potential which successfully described the mechanical properties of bulk silicon. Afterwards, Brenner and van Duin et al., developed (following a similar strategy) the so called Reactive Empirical Bond Order (REBO) [45,46] and the ReaxFF [47] reactive force fields, respectively. These RFFs were successfully used first for the study of chemical reactions between hydrocarbons and during the last decade, ReaxFF has been extensively used for many different multicomponent systems, see e.g. Ref. [48].

One of the first attempts to simulate supersonic molecular beam experiments using a RFF, was made by Ludwig et al. [49]. Using ReaxFF, they studied the dissociative adsorption of H_2 on Pt(111) and its vicinal surfaces. Their results were quite discouraging since even a qualitative agreement with the available experiments [50] was not achieved, probably due to the lack of a specific training of the ReaxFF to describe dissociation of H_2 on Pt(111). Later, Xiao et al. [34] built a Tersoff-like RFF specifically aiming at describing the interaction of H_2 with the (111), (100), and (110) faces of Pd by *training* the RFF to reproduce a large set of Density Functional Theory (DFT) interaction energies for H_2/Pd(111). The use of such a reaction specific RFF allowed for obtaining, from classical trajectory calculations, sticking probabilities in good overall agreement with previous state-of-the-art theoretical results and experiments. Interestingly, only a few months later, Valentini et al. [51] also reported classical trajectory MD results in good agreement with molecular beam experiments for O_2/Pt(111), using a ReaxFF PES specifically trained to reproduce a large set of O/Pt(111) and O_2/Pt(111) DFT interaction energies (including molecularly adsorbed states and dissociation barriers) [51].

Encouraged by these promising results we have undertaken an even more challenging task, i.e. constructing Tersoff-like RFFs for methane interacting with Pt(111) and Ni(111). It is well known that in order to investigate reactive scattering at low energies, an accurate description of the PES around the TS and in the entrance channel is necessary. In addition, an adequate description of the vibrational spectrum of methane in vacuum is also important to investigate vibrational mode-selective reactivity. Finally, for methane interacting with Pt(111) and Ni(111), it is also necessary to properly account for the effect of surface distortions (with respect to its equilibrium configuration) on the molecule–surface PES since significant surface temperature effects have been reported in particular for low energy molecules [52,30,32]. Thus, obtaining adequate RFFs for methane interacting with Pt(111) and Ni(111) fulfilling all the above requirements is certainly a big challenge. We will demonstrate this is now possible with CH_4/Pt(111) as an illustration example.

2.2. Database and fitting procedure

The formalism of RFF used for CH_4/Pt(111) is the same as that for H_2/Pd(111) we developed previously and the reader is referred to Ref. [34] for technical details. The database for fitting the RFF contains uniquely potential energies obtained from density-functional-theory (DFT) calculations. The DFT calculations for CH_4/Pt(111) were carried out with the VASP code [53,54] which uses a plane wave basis set for the electronic Kohn–Sham orbitals without spin polarization. The electronic exchange and correlation is described within the generalized gradient approximation (GGA) using the Perdew–Burke–Ernzerhof (PBE) functional [55]. The interaction of the valence electrons with the ionic cores was described within the projector augmented-wave (PAW) method [56] and the cut-off energy employed was 450 eV. The surface has been modeled by a five-layer slab and using a (3×3) unit cell with a vacuum space between consecutive slabs corresponding to six metal layers. A Monkhorst–Pack grid [57] of $5 \times 5 \times 1$ $\boldsymbol{k}$-points was used. Electronic smearing was introduced within the Methfessel–Paxton scheme [58] with $N = 1$ and $\sigma = 0.1$ eV, and the energies were then extrapolated to 0 K. The geometry of the clean surface was optimized by allowing relaxation of the two topmost layers and keeping fixed the interlayer distance between the three bottom layers at the ideal theoretical value obtained for bulk. By fully optimizing the geometry of CH_4 far from the surface we obtained a C–H distance, $r_{C-H} = 1.097$ Å, in good agreement with the experimental value of 1.085 Å [59].

To generate an initial fitting database, molecule–surface calculations have been carried out first keeping the surface *frozen* in its equilibrium structure, afterwards surface distortions were considered due to the interaction with the CH_4 molecule or due to thermal fluctuations. In the latter case, we only allowed the metal atoms in the two topmost layers to move away from their equilibrium positions for the clean surface. Unless otherwise stated, we define the zero of the molecule–surface potential energy ($V = 0$ eV), as the minimum energy obtained after fully optimizing the geometry of both CH_4 and the surface far from each other.

For the search of saddle points of the molecule-surface PES, a rough preliminary localization was carried out using the nudged elastic band (NEB) method [60–62] for optimizing typically 8 intermediate nodes until the force on each atom was smaller than 0.01 eV/Å. Then, starting from the structure with the highest potential energy obtained in each NEB calculation, a further optimization was performed using a Quasi-Newton algorithm until reaching a maximum total force on all the *mobile* atoms smaller than 0.01 eV/Å. Finally, the actual character of the saddle points was checked as usual, by diagonalizing the Hessian matrix of the PES and verifying the existence of only one imaginary frequency.

The search of the optimum values for the RFF parameters, 77 for the system considered here, is performed by using the Levenberg–Marquardt non-linear weighted least square method [63]. We have carried out a first optimization of the RFF parameters using a relatively small initial database of configurations. Then, this preliminary RFF obtained was used in classical trajectory calculations for a relatively small number of trajectories (typically 1000) for various (low, intermediate, and high) initial energies of the incident molecule. From these MD simulations, a small set of visited configurations is selected and incorporated into a new version of the database. The new extended database is then used for a re-optimization of the RFF parameters and this procedure is iteratively repeated until the RFF parameters and the sticking probabilities do not change significantly. Thus, our method to grow the configuration database is reminiscent of the Collins' group implementation of the Modified Sheppard method to build PESs [64].

2.3. Accuracy appraisal

In this feature article, we will not present an in-depth analysis for appraising in detail the accuracy of the parameterized RFF, but just illustrate its precision by comparing the RFF description of two critical regions for MD simulations, i.e. the vibrational spectrum of the methane molecule in vacuum and the neighborhood of transition states.

We have computed the vibrational spectrum of CH_4 and all its deuterated isotopomers in vacuum by diagonalizing the Hessian matrix obtained from our RFF (i.e. within the harmonic approximation) and from DFT calculations. The frequencies obtained for all the vibrational normal

modes are presented in Table 1 together with available experimental data [65]. It can be seen that the agreement with both the DFT and experimental values is excellent, discrepancies being in general, smaller than or close to 100 cm^{-1} (~0.012 eV). Moreover, the energy ordering of the various vibrational levels is well reproduced even for those which are quite close to each other. Finally, the degeneracy, λ_k, of the vibrational modes for all the isotopomers are also reproduced since they are determined by the PES symmetry properties which are properly accounted for by our RFF from definition. Thus, the developed RFFs can properly describe vibrations of CH_4 and its deuterated isotopomers in vacuum. This is a prerequisite to investigate vibrational mode-selective reactivity.

We give a second illustration concerning the reaction barrier and the transition-state (TS) structure for the methane dissociation on Pt(111). The structures of the six TSs are presented in Fig. 1 (a–f). The energetics and the main geometrical characteristics of the TSs obtained from DFT and the developed RFF are compared in Tables 2 and 3 for the rigid surface and allowing surface relaxation respectively. The search of saddle points using the RFF was carried out by minimizing the modulus of the gradient of the RFF potential energy surface, starting from the DFT TS configurations. The agreement between the obtained RFF TSs and the DFT ones is very good for both geometry and energetics. The largest deviation for the dissociation barrier is 0.03 eV for the rigid surface and 0.08 eV for the relaxed substrate, i.e. less than ~ 4% and ~ 12% errors respectively. The geometry of the DFT TSs is also well reproduced by the RFF, with the deviations for the corresponding d_{CM} and r_{CM} distances ≤0.05 Å (rigid surface) or ≤0.10 Å (relaxed substrate) and for the angle θ (see Fig. 1 g), ≤2° (rigid surface) or ≤4° (relaxed substrate). Although the overall accuracy is still very good, the quality of the RFF deteriorates slightly in the case of a relaxed surface. This might come from an analytical form of the RFF better adapted to describe covalent instead of metallic bonds. However, elucidating this requires further studies also for other metal surfaces which are in progress in our groups.

Table 1
Theoretical (harmonic) and experimental [65] normal-mode frequencies, ν_k, and degeneracies, λ_k ($\sum_k \lambda_k = 9$), for CH_4 and its deuterated isotopomers in vacuum. The theoretical results have been obtained with the RFF developed for CH_4/Pt(111) (ν_k^{RFF}) and DFT calculations (ν_k^{DFT}).

	k	λ_k	ν_k^{RFF} (cm^{-1})	ν_k^{DFT} (cm^{-1})	ν_k^{exp} (cm^{-1})
CH_4	1	1	2953.7	2987.1	2916.49
	2	2	1516.1	1513.0	1533.34
	3	3	3097.1	3090.2	3019.49
	4	3	1401.4	1287.3	1310.76
CD_4	1	1	2089.7	2112.1	2101.37
	2	2	1072.6	1070.4	1091.65
	3	3	2296.3	2285.3	2260.08
	4	3	1058.1	972.8	997.87
CH_3D	1	1	2996.3	3017.0	2969.52
	2	1	2238.5	2238.7	2200.04
	3	1	1394.0	1282.4	1306.85
	4	2	3097.0	3090.1	3016.71
	5	2	1476.4	1453.5	1472.02
	6	2	1220.5	1137.1	1161.10
CHD_3	1	1	3066.5	3068.5	2992.75
	2	1	2136.4	2151.4	2142.58
	3	1	1067.7	980.5	1004.55
	4	2	2296.4	2285.8	2250.83
	5	2	1314.8	1272.2	1292.50
	6	2	1065.4	1010.9	1035.92
CH_2D_2	1	1	3033.4	3044.3	2975.48
	2	1	2185.7	2194.2	2203.22
	3	1	1457.9	1416.9	1435.13
	4	1	1067.7	1008.0	1033.05
	5	1	1316.5	1312.1	1331.36
	6	1	3096.8	3089.9	3012.30
	7	1	1162.7	1067.4	1091.18
	8	1	2296.4	2286.2	2234.69
	9	1	1313.2	1211.8	1236.28

As far as geometry is concerned, the six DFT TSs schematized in Fig. 1 (a-f) are similar to the ones reported previously by Nave and Jackson [26]. However, the activation energies reported here are ≈100 meV smaller than those of Ref. [26]. This discrepancy is due to the different sizes of surface cell, i.e., a 3 × 3 unit cell in our work, while a 2 × 2 one in that of Nave and Jackson. In a few test calculations using a 2 × 2 cell, we have obtained a larger activation energy close to the ones reported in Ref. [26].

3. Reactive sticking of methane on Pt(111)

The aim of this paper is to illustrate, explain the origin, and predict the optimum conditions to achieve full bond selectivity taking as benchmark system, the reactive sticking of partially deuterated isotopomers of methane on Pt(111). For such a complete analysis we feel it is first convenient to illustrate the effect of translational energy, and surface temperature on the initial sticking probability of CH_4 in its ground ro-vibrational state as done in Section 3.1. Then, in Section 3.2 we explain how and why reactivity progressively changes when H atoms are replaced by D atoms, as well as the reactive sticking enhancement due to mode specific vibrational excitation of CH_4 and its partially deuterated isotopomers. Finally, in Section 3.3 we show how all together, these aspects allow: i) to understand the origin of full C–H bond selectivity observed experimentally, and ii) to predict the experimental conditions under which full C–D bond selectivity (not yet observed experimentally) should be also achieved. During the last years many theoretical studies have been focused on the dissociation dynamics of methane on Pt(111). Nevertheless, to our knowledge there has been no literature for such complete theoretical systematic analysis of the dissociation dynamics for all the isotopomers of methane based on a full dimensional system modelization (fifteen molecular DOFs, at least). In this paper we mainly focus on theoretical results we have recently obtained thanks to the development of the accurate RFF described in detail in Ref. [66] and briefly summarized here in Section 2. The scattering of (initially non-rotating) molecules from Pt(111) was investigated through QCMD calculations. The initial values of the internal coordinates and momenta of the atoms of the molecule for particular initial vibrational states were selected using the standard procedure described in detail in Ref. [67]. As usual, the initial molecular orientation and impact point on the surface were chosen randomly. For each initial condition, we have generated between 10^4 and 3×10^5 trajectories depending on the value of the sticking probability in order to obtain statistically well converged results. The initial coordinates and momenta of the metal atoms for each trajectory were randomly taken from a large set of *snapshots* produced during a NVT-MD simulation of the clean slabs for the considered temperature in each case. Additional information about the QCMD simulations can be found in the Supporting Information of Ref. [36]. Full dimensional AIMD calculations addressing bond selectivity have been recently reported but only for CHD_3/Pt(111) [39] and so, we will compare with AIMD results for this particular system only. Results of previous lower-dimensional and only-one-active-bond quantum and classical dynamical studies focused on CH_4 on Pt(111), Ni(111) and Ni(100) can be found in Refs. [25–27,29], and for a review the readers might see Ref. [68].

3.1. Reactivity of the "ground-vibrational-state"

In Fig. 2 we show theoretical initial reactive sticking probabilities, S_0, as a function of the translational energy, E_{trans}, compared with available supersonic molecular beam experimental data (for normal incidence). In spite of some quantitative discrepancies, all the set of experimental data exhibit a strong increase of S_0 when E_{trans} increases, typical for a direct activated dissociation process. It is important to note that these sets of experimental data have been obtained (along the last ~25 years by several groups) using different methods, and for different surface and nozzle temperatures, and so, discrepancies are not unexpected. On the one hand, in what extent discrepancies are due to the different

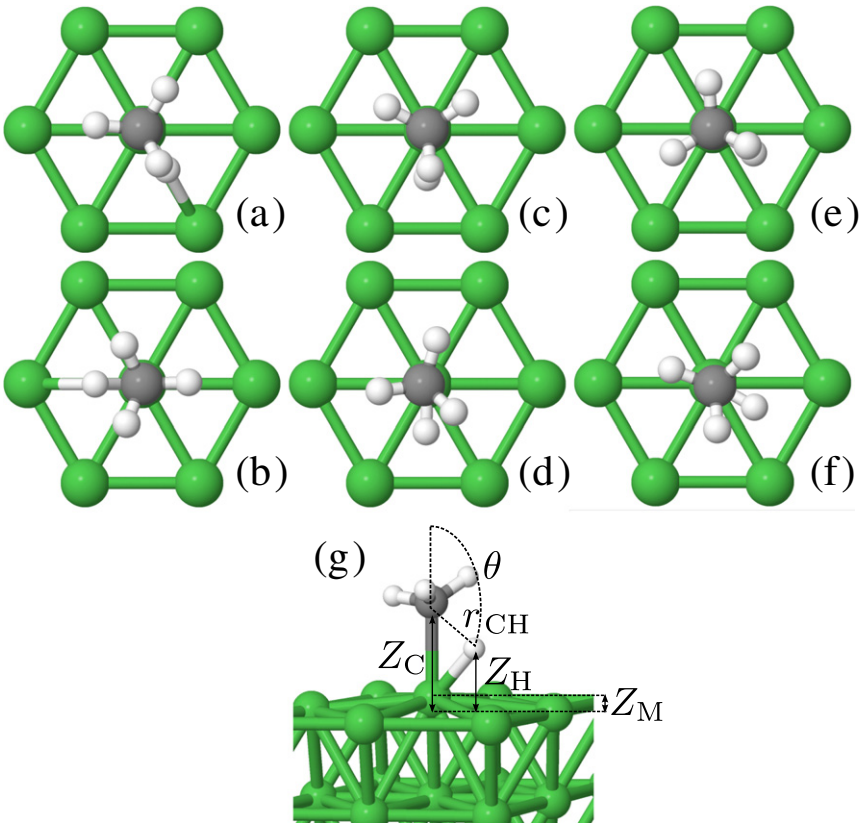

Fig. 1. (a–f) Top view of different TS structures found for CH_4 dissociation. (g) Side view of a typical TS on a relaxed surface, and coordinates used to characterize it. *Z* coordinates relative to topmost layer at equilibrium configuration (0 Å).

experimental methods (including not only the one used to determine S_0 but also the sample preparation and cleaning) cannot be easily evaluated. On the other hand, both higher surface and nozzle temperatures, are expected to entail higher S_0 values, in the latter case, due to a larger population of molecules with higher internal energies in the molecular beam. In line with this, the S_0 values measured by Luntz and co-workers (red and magenta squares) [52,30] for $T_s = 800$ K are higher than the ones obtained by the Beck's group (black circles) for $T_s = 150$ K [69], and lower than those found by the Madix's group (blue triangles) for a higher nozzle temperature, T_n [70].

Though some ro-vibrational excited molecules (whose fraction is not always precisely known) do exist in the beams, it is still meaningful to compare the experimental data of Fig. 2a with calculations for the ro-vibrational ground state (gs) of CH_4, CH_4(gs). The black and red lines depicted in Fig. 2a correspond to calculations for $T_s = 150$ K and 800 K, i.e. the lowest and highest temperatures considered in experiments respectively. Theoretical $S_0(E_{trans})$ curves for intermediate T_s values (not shown) lie between the ones reported in Fig. 2a. Our MD calculations predict too large S_0 values compared with experiments for both surface temperatures similar to the findings of Mastromatteo and Jackson [71] for methane dissociation on Ni(111) and Ni(100). In the present case, the agreement with experiments is better for $T_s = 800$ K, in particular for $E_{trans} \leq 0.5$ eV. This might be due to some error cancelation, e.g., due to an overestimation of the reactivity at low surface temperatures, and underestimation of the promoting T_s-effect. Still, the agreement with experiments is quite satisfying. This is so in particular, if one takes into account the complexity of this high dimensional system, and that no adjustable parameters and/or extra approximations (beyond the use of classical mechanics to describe the dynamics) have been made after setting up the RFF purely based on DFT results.

For $T_s = 150$ K, the experimental values can be reproduced well by shifting to the right the corresponding theoretical $S_0(E_{trans})$ curve by ~0.13 eV. This might indicate that the activation energy barriers of the RFF employed in the present simulations are (in average) too large by ~0.13 eV. Taking into account that the RFF underestimates the

Table 2
Activation energy barrier for dissociation, E_b, and the TS geometry as shown in Fig. 1 for CH_4 on a rigid Pt(111) surface, obtained in DFT calculations and with the developed RFF (ε: absolute value of the discrepancy between the DFT and RFF E_b values).

	DFT				RFF				
	d_{CM} (Å)	r_{CH} (Å)	θ (°)	E_b (eV)	d_{CM} (Å)	r_{CH} (Å)	θ (°)	E_b (eV)	ε (eV)
a	2.24	1.51	131	0.81	2.23	1.53	131	0.83	0.02
b	2.25	1.50	132	0.82	2.26	1.44	134	0.80	0.02
c	2.24	1.55	131	0.84	2.25	1.50	132	0.82	0.02
d	2.25	1.52	132	0.86	2.27	1.46	133	0.83	0.03
e	2.24	1.53	131	0.83	2.25	1.49	133	0.81	0.02
f	2.26	1.50	133	0.85	2.27	1.48	132	0.83	0.02

Table 3
Idem Table 2 but allowing surface relaxation.

	DFT					RFF					
	d_{CM} (Å)	r_{CH} (Å)	θ (°)	ΔZ_M (Å)	E_b (eV)	d_{CM} (Å)	r_{CH} (Å)	θ (°)	ΔZ_M (Å)	E_b (eV)	ε (eV)
a	2.21	1.50	131	0.17	0.68	2.19	1.46	132	0.18	0.62	0.06
b	2.23	1.47	132	0.16	0.69	2.22	1.38	134	0.16	0.63	0.06
c	2.20	1.52	132	0.17	0.71	2.21	1.42	133	0.16	0.63	0.08
d	2.22	1.50	133	0.18	0.72	2.22	1.40	133	0.16	0.65	0.07
e	2.21	1.51	133	0.17	0.69	2.20	1.45	132	0.18	0.62	0.07
f	2.23	1.48	135	0.16	0.71	2.22	1.42	131	0.19	0.63	0.08

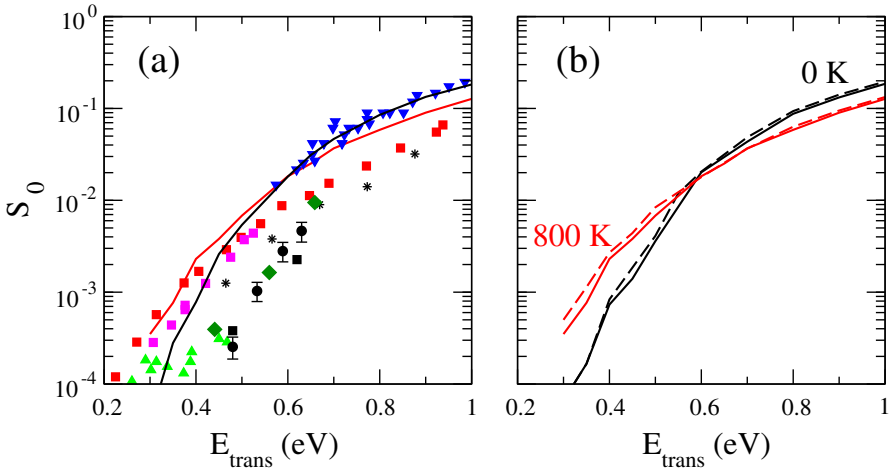

Fig. 2. Initial reactive sticking probability, S_0 as a function of the molecular translational energy, E_{trans}, for CH_4/Pt(111) at normal incidence. a) Theory: black line, $T_s = 150$ K; red line, $T_s = 800$ K. Experiments: black circles, $T_s = 150$ K [69]; black squares, $T_s = 200$ K [30]; blue down triangles, $T_s = 500$ K [70]; green up triangles, $T_s = 575$ K [72]; green diamonds, $T_s = 600$ K [73]; black stars, $T_s = 600$ K [74]; magenta squares, $T_s = 800$ K (nozzle temperature: 300 K) [52], red squares, $T_s = 800$ K (nozzle temperature: 680 K) [52]. b) Theory for $T_s = 0$ K (black lines) and 800 K (red lines): full lines, standard MD simulation; dashed lines, MD simulation using the SDS model (see text).

DFT–PBE activation energy barriers by between ~0.02 eV and ~0.07 eV (see Tables 2 and 3), this might indicate that DFT–PBE activation energy barriers are too low by between ~0.06–0.11 eV which are possible errors for such semi-local exchange-correlation density functional. This estimation is consistent with that of Nattino et al. based on a similar overestimation of experiments obtained for their AIMD results (also using the PBE functional) for CHD_3/Pt(111) [39]. We will come back to this point later in the light of the comparison with experiments for initial vibrationally excited states of CH_4.

Concerning T_s-effects, the experimental E_{trans}-dependence of S_0 for $T_s = 150$ K and 800 K are both well reproduced by theory, in particular, the decreasing slope of the $S_0(E_{trans})$ curve when T_s increases. Moreover, the promoting T_s-effect unambiguously observed experimentally for low translational energies is reproduced for $E_{trans} \leq 0.6$ eV, though the T_s-effect predicted theoretically seems to be smaller than the one observed experimentally. For higher impact energies, our calculations predict a decrease of S_0 for increasing T_s in contrast with the Luntz group experimental data that still predict an increase of S_0 with T_s but much less pronounced than for low impact energies. However, it is interesting to note that in contrast with the latter experimental results, Schoofs et al. could not observe any T_s-effect on S_0 ($E_{trans} = 0.7$ eV) between T_s ~ 500 K and 1250 K which is consistent with our theoretical results if one takes into account the estimated error bars that affected the experiments [70]. Apart from the latter two sets of experimental data, to our knowledge there is no further systematic studies of T_s-effects for large initial translational energies and so, further studies for methane/Pt(111) on this respect would be welcome.

In order to explain the origin of the T_s-effects predicted by our MD calculations, in Fig. 2b we show the results of two MD calculations. The full lines correspond to standard MD calculations (as shown in panel a) whereas the dashed lines represent the results obtained by keeping fixed the surface atoms in their initial positions (chosen in the same way as in the standard MD calculation) during the molecule–surface collision. The latter calculations will be hereafter referred to as Static Distorted Surface (SDS) model that represents a lattice-sudden approximation of the molecule–surface dynamics with metal atoms being static in a set of distorted surface configurations determined by the temperature. In Fig. 2b we present results of both kind of MD simulations for $T_s = 0$ K (black lines),[1] and $T_s = 800$ K (red lines). The very good agreement between the results obtained within the SDS model and the standard MD calculations for both temperatures clearly illustrates the moderate dynamical coupling between the molecular and surface DOFs during the fast direct CH_4/Pt(111) collision. This is due to the different time scales of the C and H atoms on the one hand (e.g. typical dissociation times are smaller than 0.2 ps [39]), and the heavy Pt atoms on the other. Thus, the T_s-effects observed in Fig. 2a are largely due to the distorted initial configurations that surface atoms adopt when T_s increases. This conclusion, is expected to be valid also for other surfaces made of heavy metal atoms, in line with previous calculations for CH_4/Ni(111) [75] and in contrast with the initial thought that collision-induced surface rearrangement could be highly effective producing a reactivity enhancement [76]. For any given T_s value, in SDS calculations we have taken the same set of initial surface distorted configurations for different impact energies. There are obviously configurations that are more reactive and other less reactive than the equilibrium surface structure (the one used for all the trajectories in calculations for $T_s = 0$ K). Since, for low and high E_{trans} values, we obtain different T_s-dependences of S_0, it is clear that the features of the PES that determine the effect of T_s on S_0 changes with E_{trans}. Our MD results show that for low (high) E_{trans} values, the distorted surface configurations more (less) reactive than the equilibrium one, are the ones that prevail.

3.2. Isotopic effect, vibrationally enhanced reactivity and mode-specificity

Before considering bond selectivity for partially deuterated isotopomers of methane, it is convenient to understand the reactivity changes due to the successive replacement of H atoms by D atoms in the CH_4 molecule. Therefore, Fig. 3a shows theoretical results of S_0 as a function of E_{trans} for $CH_{4-x}D_x$(gs) ($x = 0,1,2,3,4$) for $T_s = 150$ K. It is observed that S_0 decreases when the number of D atoms, x, increases. Up to our knowledge, a comparative experimental study of the reactivity of $CH_{4-x}D_x$ ($x = 0,1,2,3,4$) on Pt(111) has not been reported yet and so, this trend waits for an experimental confirmation. Still, such monotonously decreasing reactivity of deuterated isotopomers of methane when the number of D atoms increases has been observed on tungsten surfaces [77]. In addition, a lower reactivity of CD_4 compared to that of CH_4 has been reported before not only for Pt(111) [52] but also on other metal surfaces [32]. At this point it is interesting to mention that our results for CHD_3/Pt(111) are in good agreement with the values obtained by Nattino et al. [39] for 0.75 eV ≤ E_{trans} ≤ 0.85 eV which represents a further validation of our RFF.

[1] For $T_s = 0$ K, the SDS model corresponds to what is usually called, rigid surface approximation in which surface atoms are kept fixed in their equilibrium positions for the clean surface.

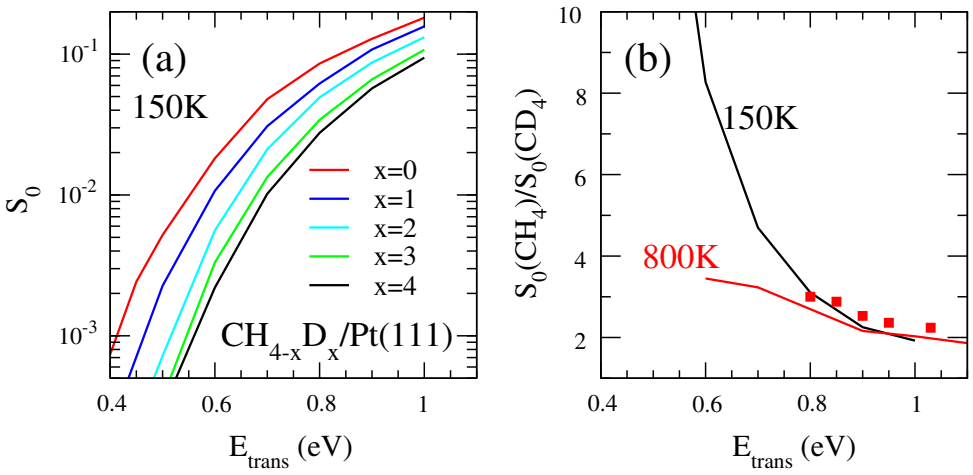

Fig. 3. a) Initial reactive sticking probability, S_0, as a function of the molecular translational energy, E_{trans}, for $CH_{4-x}D_x$/Pt(111) ($x = 0,1,2,3,4$) and $T_s = 150$ K. b) Ratio of reactive sticking probabilities $S_0(CH_4)/S_0(CD_4)$ for $T_s = 150$ K (black line) and $T_s = 800$ K (red line). Red squares: experimental data for $T_s = 800$ K [52].

In a calculation for an *artificial* CD_4 molecule with the same vibrational zero point energy as CH_4, it is obtained a sticking curve much closer to the one of CH_4: smaller only by a factor of ~0.83 than [36]. This indicates that the isotopic effect illustrated in Fig. 3a is largely due to the decrease of the ZPE of $CH_{4-x}D_x$(gs) when x increases, and the relatively high vibrational efficacy that characterizes methane dissociation on Pt(111) as well as on many other metal surfaces [8,78]. The increase of the ZPE roughly produces a horizontal shift of the $S_0(E_{trans})$ curve to the left, i.e. towards lower E_{trans} values. This energy shift and the strong increase of S_0 for increasing E_{trans} at low energies, are the reasons for a ratio $S_0(CH_4)/S_0(CH_{4-x}D_x)$ increasing when E_{trans} decreases (more pronounced for the more deuterated isotopomers). In Fig. 3b we have plotted the ratio $S_0(CH_4)/S_0(CD_4)$ as a function of E_{trans}, for $T_s = 150$ K and 800 K. The theoretical results agree very well with the ratio measured by Luntz and co-workers for $T_s = 800$ K which monotonously decreases from ~3.3 to 2.5, for 0.8 eV ≤ E_{trans} ≤ 1.2 eV, i.e. an energy range for which this ratio barely depends on T_s. However, for $T_s = 150$ K the increase of the ratio $S_0(CH_4)/S_0(CD_4)$ for decreasing E_{trans} is much more pronounced than for $T_s = 800$ K. This is due to the smaller slope of the $S_0(E_{trans})$ curves when T_s increases already discussed on the light of the results of Fig. 2a. This shows that the role of vibrational energy on reactivity is not only more prominent at low translational energies but also at low surface temperatures.

Experimentally, it has been shown that the efficacy of the initial vibrational energy to activate the C–H bond cleavage depends on the particular mode that is excited (see Refs. [78,9,7] and Ref. [79] for a review). For instance, Beck and co-workers have found for Ni(100) [9], that the reactivity of CH_4 vibrationally excited in the symmetric stretching mode $1\nu_1$, is higher than for CH_4 initially excited in the asymmetric stretching mode $1\nu_3$, in spite of the slightly lower internal energy of $CH_4(1\nu_1)$. In addition, Beck and co-workers have also found that CH_2D_2 in a state excited with two quanta of vibration in the same stretching mode, is more reactive (by a factor of ~5) than for an excited state with two vibrational quanta each one in a different mode [7], in spite of the very similar internal energies of both excited states. This shows that methane dissociation on metal surfaces is in general, mode-specific.

In order to illustrate mode-specificity in reactive sticking of CH_4 on Pt(111), in Fig. 4a we have plotted the $S_0(E_{trans})$ curves for various vibrationally excited initial states of CH_4: $1\nu_2 + 1\nu_4$, $1\nu_1$, $1\nu_3$, and $3\nu_4$. From Table 1, it can be seen that the excitation energy values of the latter states are (in cm^{-1}): 2917.5, 2953.7, 3097.1, and 4204.2 respectively. Whereas, ν_1 and ν_3 are both stretching modes (symmetric and asymmetric respectively), ν_2, and ν_4 are both bending modes. Comparing the sticking curves for bending modes on one side and stretching modes on the other, it is clear that the latter are much more efficient promoting bond breaking than the former. On the one hand, the $1\nu_2 + 1\nu_4$ state has almost the same internal energy as the $1\nu_1$ state but the reactivity of the latter is significantly larger. On the other hand, the $3\nu_4$ state has an excitation energy ~42% (~0.15 eV) higher than the $1\nu_1$ state but the reactivities of both states are very close to each other. Comparing the vibrational efficacy of both stretching modes, the symmetric $1\nu_1$ state is slightly more reactive than the asymmetric $1\nu_3$ one in spite of being slightly less energetic. Though (to our knowledge) the reactive sticking probability of $CH_4(1\nu_1)$ has not been measured on Pt(111), it is interesting to recall the previously mentioned result, that a reactivity $CH_4(1\nu_1)$ higher than that of $CH_4(1\nu_3)$ has been reported for Ni(100) [9] in line with our theoretical results. Also important is the fact that the mode-specificity put in evidence experimentally, is also predicted by theory.

Concerning the comparison with experiments, in Fig. 4a we have also included experimental data from the group of Beck for $CH_4(1\nu_3)$ which agree very well with the corresponding theoretical results. This agreement might be indicating that the too large reactivity predicted for CH_4(gs) (see Fig. 2) could be due to a limitation of the quasi-classical method to sample the ground state of CH_4 (alleviated for vibrationally excited states), instead of being an indication of too low DFT–PBE activation energy barriers as mentioned above. To clarify these issues further theoretical and experimental investigations are probably necessary.

An important general aspect of methane reactivity on Pt(111) illustrated in Fig. 4a, is that being significantly vibrational mode-specific, intramolecular vibrational redistribution (IVR) is not so relevant as could be anticipated given the large number of molecular DOFs. This shows on the one hand, that statistical methods considering only the total internal energy of the molecule to predict the reactivity for a given E_{trans} value cannot be applied to simulate supersonic molecular beam experiments. On the other hand, it also shows that typical collision times are shorter than the characteristic time for vibrationally de-excitation through energy exchange with phonons and/or by electron-hole pair excitations, most likely due to dissociation being fast and decided relatively far from the surface (e.g. the C height above the surface at the TSs is larger than 2.2 Å, see Tables 2 and 3).

Now it is important to consider the effect of vibrational excitation for the partially deuterated isotopomers of methane. In Fig. 4b we compare the $S_0(E_{trans})$ curve for $CH_4(1\nu_3)$ with those for $CH_3D(1\nu_4)$, $CH_2D_2(1\nu_6)$, and $CHD_3(1\nu_1)$, i.e. for first excited state corresponding to the most energetic stretching mode of all the partially deuterated isotopomers of CH_4. Interestingly, in spite of the significant reactivity differences

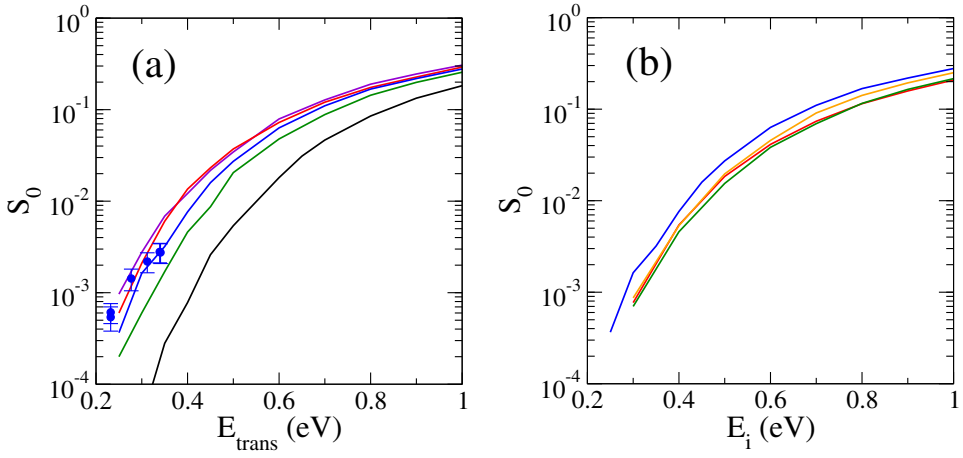

Fig. 4. a) Reactive sticking probability, S_0, as a function of the molecular translational energy, E_{trans}, for CH_4 (in various vibrational initial states) on Pt(111) for $T_s = 150$ K. Theory: black line, ground state; green line, $1\nu_2 + 1\nu_4$ state; blue line, $1\nu_3$ state; red line, $1\nu_1$ state; violet line, $3\nu_4$ state. Experiments: blue circles, $1\nu_3$ state from Ref. [69]. b) Idem a) but for $CH_4(1\nu_3)$ (blue line), $CH_3D(1\nu_4)$ (orange line), $CH_2D_2(1\nu_6)$ (green line), and $CHD_3(1\nu_1)$ (red line).

between the partially deuterated isotopomers in the ground state (Fig. 3a), for the vibrationally excited states considered in Fig. 4b, the reactivities are very close to each other and also relatively close to that of $CH_4(1\nu_3)$. This means that vibrational efficacy for these excited states increases when the number of D atoms, *x*, increases. This is connected with the fact that the latter are all C–H stretching modes and when *x* increases, the vibrational excitation energy is more focused on fewer C–H bonds which would favor the bond cleavage. This is probably due to a larger projection of the corresponding normal mode onto the reaction coordinate near the TS.

3.3. Bond-selective reactivity

Achieving high selectivity is one of the major goals in catalysis because this allows for producing preferentially the desired products [80]. Therefore, elucidating and controlling the factors that promote the cleavage of a specific bond of a polyatomic molecule is of great fundamental importance and tremendous practical usefulness. The challenge of bond selectivity with $CH_{4-x}D_x$ is the ability of selecting the cleavage of C–H or C–D bond, despite their same activation energy (neglecting ZPE effects). Thus, a branching ratio of C–H (or C–D) cleavage similar to the fraction of C–H (or C–D) bonds in the molecule corresponds to a *statistical* (or weak) selectivity, whereas *full* selectivity is attained if only one type of bond (C–H or C–D) is cleaved. By exciting with a laser a C–H stretching mode of $CH_{4-x}D_x$ ($x = 1,2,3$) before the collision with Pt(111) (E_{trans} ~ 0.25 eV), it was achieved full C–H bond selectivity in contrast with a weak selectivity found under laser-off conditions for molecules with the same total energy (E_{trans} ~ 0.55 eV) [11]. Fig. 5 shows that the theoretical C–H branching ratios are in excellent agreement with the latter experimental data for all the partially deuterated isotopomers of methane. For CHD_3(gs), CH_2D_2(gs), and CH_3D(gs), the branching ratios are close to the statistical values, whereas fully selective cleavage of C–H bonds is achieved for $CHD_3(1\nu_1)$, $CH_2D_2(1\nu_6)$, and $CH_3D(1\nu_4)$ on Pt(111).[2]

Due in part to the high complexity of bond selectivity measurements, such studies [10,11] have been hitherto performed for very particular experimental conditions. Thus, it is interesting to predict theoretically, how bond-selectivity varies as a function of the molecular translational energy and surface temperature. In Fig. 6, we report the theoretical branching ratios of the C–H bond cleavage on Pt(111) for CHD_3(gs) and $CHD_3(1\nu_1)$ (panel a), CH_2D_2(gs) and $CH_2D_2(1\nu_6)$ (panel b), and CH_3D(gs) and $CH_3D(1\nu_4)$ (panel c), as a function of E_{trans}. It is observed that the high C–H bond selectivity observed in Fig. 6 decreases with increasing E_{trans}, the C–H branching ratios approaching the statistical value. Though to our knowledge, the E_{trans}-dependence of bond selectivity has not been investigated through state-resolved-reactivity experiments for partially deuterated isotopomers of methane interacting with surfaces, it is interesting to mention that a similar loss of selectivity has been observed in bimolecular reactions [81,82].

The loss of bond selectivity with increasing E_{trans} is a consequence of the fact that translational energy is not bond selective. At high translational energies the molecules can approach closer to the surface and vibrational softening is strongest: the typical Morse-like effective C–X (X = H or D) interaction potential far from the surface (e.g. for Z_C = 4 Å), tends to become purely repulsive close to the surface (e.g. for Z_C = 2.2 Å) when the atoms start forming new bonds with the metal (see Fig. 7). Thus, when E_{trans} increases, the bond most likely to be cleaved (more and more irrespective of the vibrational energy initially stored in it) is that most involved in the molecule–surface interaction, i.e., the one most favorably oriented for dissociation near the point of closest approach to the surface. Then, the loss of bond selectivity induced by stretching at high E_{trans} can be explained, on the one hand, by the non-selective character of the translational energy and, on the

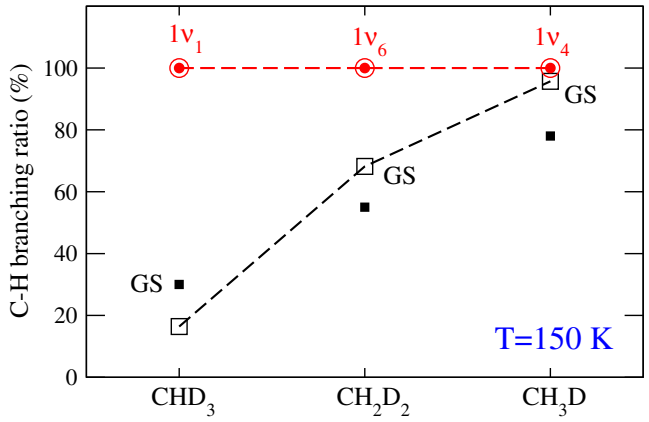

Fig. 5. Branching ratio of C–H bond cleavage for $CH_{4-x}D_x$/Pt(111) ($x = 1,2,3$). Open symbols represent the theoretical results of this work and filled symbols the experimental data from [11]. Circles: vibrationally excited molecules (vibration mode indicated near the corresponding data) for $E_i = 0.25$ eV; squares: molecules in the vibrational GS (under laser-off conditions in the case of experiments) for $E_i = 0.55$ eV. Dashed lines connecting theoretical results are plotted to guide the eyes.

[2] Similar results have been also found experimentally [10] for Ni(111) and properly reproduced later by theory [36].

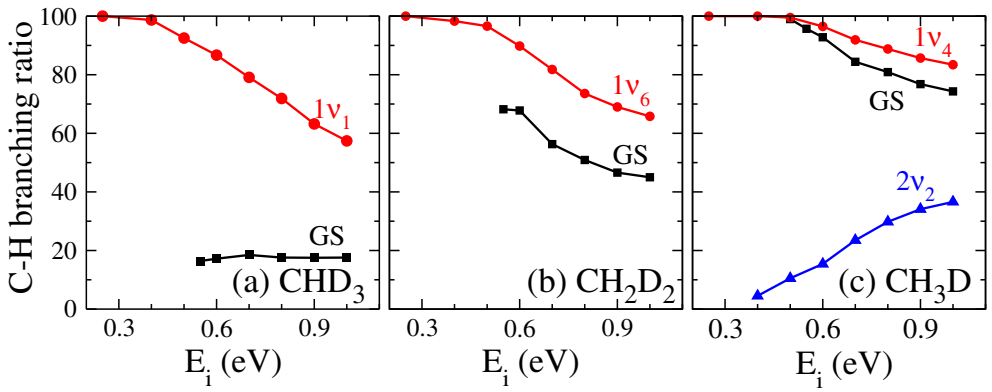

Fig. 6. C–H branching ratio as a function of E_{trans} for $CH_{4-x}D_x$/Pt(111) for various initial vibrational states. a) $x = 3$, b) $x = 2$, c) $x = 1$.

other hand, by the decreasing role of the initial vibrational energy when E_{trans} increases. In addition, some loss of selectivity for increasing impact energies might be also due to an energy transfer from the initially excited vibrational mode to the others which might be more favored at high impact energies for which molecules tend to approach closer to the surface where the coupling between vibrational modes is stronger. In any case, theoretical results indicate that the mode-specific high selectivity observed experimentally in Ref. [11] would be due, to a large extent, to the low translational energies considered. Under such conditions, the vibrational energy initially deposited in a stretching mode promotes more efficiently the corresponding bond(s) scission than the non-bond-selective translational energy.

Since we have shown that the conditions under which strong bond-selectivity can be achieved are the ones for which vibrationally-enhanced reactivity is most prominent, in view of the results of Fig. 3b one suspects that bond-selectivity might be also reduced for increasing T_s (though less dramatically than with increasing E_{trans}). Interestingly, this has been confirmed by MD simulations for $CHD_3(1\nu_1)$ and $E_{trans} = 0.4$ eV for $T_s = 800$ K for which we have obtained a C–H branching ratio equal to 88%, in contrast with the 99% value obtained for $T_s = 150$ K (Fig. 6a).

Before concluding, it is important to mention that full selectivity has been so far experimentally achieved only for the cleavage of C–H bonds. Whether and how fully selective cleavage of the *less active* C–D bond can be realized remains an open issue. Hence, it is interesting to investigate the possibility of such a selective cleavage, in particular for the most statistically unfavorable case, i.e., CH_3D. Therefore, we have computed $S_0(E_{trans})$ for $CH_3D(1\nu_2)$ and $CH_3D(2\nu_2)$ on Pt(111) (ν_2 being a localized C–D stretching mode of CH_3D). In both cases, an increased C–D bond selectivity (i.e. a decrease of the C–H branching ratio) is observed. Though full C–D selectivity cannot be reached for $CH_3D(1\nu_2)$ (results not shown), our simulation predicts that the full C–D selectivity can be

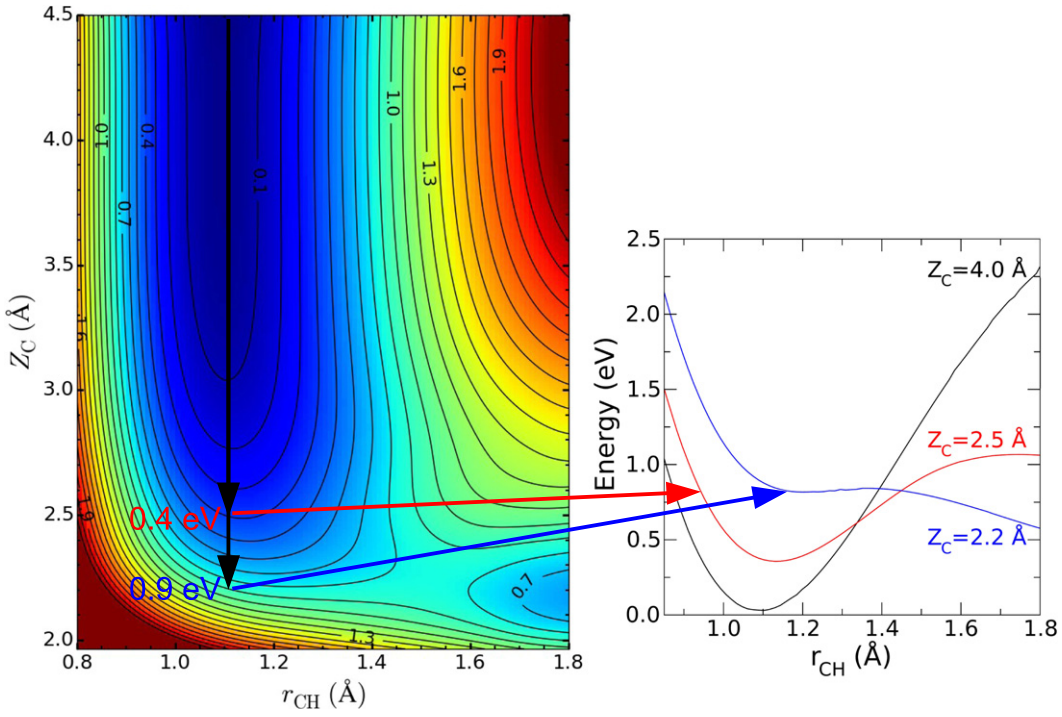

Fig. 7. On the left, contour plot of a two-dimensional (2D) cut of the methane/Pt(111) PES as a function of Z_C and r_{CH} (see Fig. 1) for the C atom kept fixed on top of a Pt atom (within a rigid surface model) and after optimizing all the remaining eleven molecular coordinates. Contour spacing: 0.1 eV. On the right, r_{CH}-dependence of the extracted from the 2D cut of the methane/Pt(111) PES on the left for $Z_C = 4.0$ Å (black line), 2.5 Å (red line), and 2.2 Å (blue line). The latter Z_C values have been chosen to illustrate the r_{CH}-dependence far from the surface, and classical turning points for molecules impinging the surface with $E_{trans} = 0.4$ eV, and 0.9 eV respectively (see text).

achieved with the first overtone of ν_2, i.e., $CH_3D(2\nu_2)$, for $E_{trans} \lesssim 0.4$ eV (see the blue curve in Fig. 6c). Again, under such a condition, the effect of mode-specific vibrational excitation prevails over the non-selective translational energy. We hope that this prediction will stimulate further experimental investigations of bond selectivity on metal surfaces.

4. Conclusions and perspectives

In this paper, we have presented our recent work on a benchmark system for polyatomic-molecule surface reactions, methane/Pt(111), in order to gain some new insight into bond-selective reactivity revealed recently by gas–surface supersonic molecular beam experiments. The new results from state-of-the-art molecular dynamics simulations based on Density Functional Theory (DFT) calculations are compared with available experimental data. We have briefly described a divide-and-conquer approach through which it is possible to build a reaction specific reactive force field capable of accounting for the high dimensional potential energy landscape for polyatomic molecules interacting with metal surfaces from DFT total energy data. This approach allows now for performing full-dimensional quasi-classical trajectory calculations in which not only all the fifteen degrees of freedom (DOF) of methane have been treated on an equal footing, but also the coupling with the DOFs of metal atoms is accounted for during the dynamics simulation.

In the light of the outcome of such MD simulations and the comparison with vibrational-state-resolved supersonic molecular beam experiments, we have discussed various aspects of vibrationally-enhanced-mode-specific and bond-selective reactivity of CH_4 and its deuterated isotopomers with the focus on the way that translational and vibrational energy, as well as surface temperature influence both, global reactivity and bond selectivity. We have illustrated how translational energy efficiently activates the first bond cleavage of methane on metal surfaces and the prominent role of vibrational energy, in particular at low translational energies for which the sticking probability is small. We have shown that the latter is in fact, the main responsible for the isotopic effect observed when comparing the sticking curves for the methane isotopomers, $CH_{4-x}D_x$(gs) on Pt(111) ($x = 0,1,2,3,4$), molecules with larger vibrational zero point energy (ZPE) being more reactive. However, not only the vibrational energy matters since, stretching modes whose projections onto the reaction coordinates near the transition state are larger, are largely more efficient than bending modes for promoting reactive sticking. Thus, methane dissociation is mode specific, due to the short collision times (typically $\lesssim 0.2$ ps) with respect to the time scale for intramolecular vibrational redistribution (IVR). The relative importance of initial vibrational energy decreases when the molecular translational energy E_{trans} increases basically because faster molecules can approach closer to the surface and reach a region of configuration space where the C–H interaction becomes purely repulsive and so, the initial vibrational energy stored in this bond becomes less relevant for the bond breaking process. This entails in particular a decrease of (mode-specific) vibrationally induced bond selectivity when E_{trans} increases. Finally, we have also illustrated how the large mass mismatch between the H and C atoms on one hand and Pt atoms on the other, results in a weak dynamical coupling between the molecular and surface DOFs during the fast direct dissociation process. This is not inconsistent with significant surface temperature effects on reactivity, which are mainly due to the larger set of distorted surface configurations that molecules can encounter when T_s increases. In particular, at low translational energies where the sticking probability is largely influenced by the lowest activation energy barrier offered by the thermally distorted surface, the increase of T_s always promotes reactivity. Such higher reactivity entails also some decrease of the role of initial (mode-specific) vibrational motion and so, bond selectivity is expected to slightly decrease when T_s increases. Thus, our calculations predict that bond selectivity is more likely to be achieved taking advantage of the mode-specific vibrationally enhanced reactivity, mainly for low translational energies and secondly, for low surface temperatures. We do hope that these predictions will motivate new experiments aimed to check the validity of such conclusions. Also, welcome are further developments of high dimensional quantum dynamics calculations since, in spite of the great power of the quasi-classical trajectory method, issues like the so-called ZPE violation problem, including artificially enhanced IVR process cannot be completely ruled out.

About fifteen years ago, the advent of then new interpolation strategies for building PES allowed a significant step forward towards accurate molecular dynamics simulations of dissociation of diatomic molecules on metal surfaces. The reaction specific reactive force fields as that illustrated in this paper should be able to open the door towards similar achievements for polyatomic molecules. It can be expected that new methodological developments in this direction as well as higher dimensional quantum dynamics methods in progress today will allow, in a near future, for making significant advances for understanding better the dynamics of polyatomic molecules on metal surfaces. We do hope, of course, that the combined efforts of such theoretical developments and further experimental investigations will not leave Maxwell demon alone to explore the new fascinating forefronts in surface chemical reactions.

Acknowledgments

We thank the ECOS-Sud program (project A11E06) for financial support. X. J. S. thanks China postdoctoral Science Foundation (Project 2014M551130) for financial support. W. D. thanks ANR for financial support through the Dyquma project (ANR-10-BLAN-0720) . A. L. and H. F. B. acknowledge MINCyT, (Project PICT Bicentenario 1962), CONICET, (Project PIP 0667), and UNR (Project PID ING235) for financial support.

References

[1] J.H. Larsen, I. Chorkendorff, Surf. Sci. Rep. 35 (5-8) (1999) 163 (URL http://www.sciencedirect.com/science/article/pii/S0167572999000096.).
[2] J.R. Rostrup-Nielsen, J. Sehested, J.K. Nørskov, Hydrogen and Synthesis Gas by Steam- and CO_2 Reforming, 47Academic Press, 2002. 65 (URL http://www.sciencedirect.com/science/article/pii/S036005640247006X).
[3] M.B. Lee, Q.Y. Yang, S.T. Ceyer, J. Chem. Phys. 87 (5) (1987) 2724 (URL http://link.aip.org/link/?JCP/87/2724/1).
[4] X. Li, C.W. Magnuson, A. Venugopal, R.M. Tromp, J.B. Hannon, E.M. Vogel, L. Colombo, R.S. Ruoff, J. Am. Chem. Soc. 133 (9) (2011) 2816.
[5] Y.S. Kim, J.H. Lee, Y.D. Kim, S.-K. Jerng, K. Joo, E. Kim, J. Jung, E. Yoon, Y.D. Park, S. Seo, S.-H. Chun, Nanoscale 5 (2013) 1221.
[6] L. Juurlink, P. McCabe, R. Smith, C. DiCologero, A. Utz, Phys. Rev. Lett. 83 (1999) 868.
[7] R.D. Beck, P. Maroni, D.C. Papageorgopoulos, T.T. Dang, M.P. Schmid, T.R. Rizzo, Science 302 (5642) (2003) 98 (URL http://www.sciencemag.org/content/302/5642/98.abstract).
[8] R.R. Smith, D.R. Killelea, D.F. DelSesto, A.L. Utz, Science 304 (5673) (2004) 992 (URL http://www.sciencemag.org/content/304/5673/992.abstract).
[9] P. Maroni, D. Papageorgopoulos, M. Sacchi, T. Dang, R. Beck, T. Rizzo, Phys. Rev. Lett. 94 (2005) 246104, http://dx.doi.org/10.1103/PhysRevLett.94.246104.
[10] D.R. Killelea, V.L. Campbell, N.S. Shuman, A.L. Utz, Science 319 (5864) (2008) 790 (URL http://www.sciencemag.org/content/319/5864/790.abstract).
[11] L. Chen, H. Ueta, R. Bisson, R.D. Beck, Faraday Discuss. 157 (2012) 285.
[12] V.A. Ukraintsev, I. Harrison, J. Chem. Phys. 101 (2) (1994) 1564.
[13] H.L. Abbott, A. Bukoski, I. Harrison, J. Chem. Phys. 121 (8) (2004) 3792 (URL http://scitation.aip.org/content/aip/journal/jcp/121/8/10.1063/1.1777221).
[14] S.B. Donald, J.K. Navin, I. Harrison, J. Chem. Phys. 139 (21) (2013) 214707.
[15] G.R. Darling, S. Holloway, Rep. Prog. Phys. 58 (12) (1995) 1595.
[16] A. Gross, M. Scheffler, Phys. Rev. B 57 (1998) 2493, http://dx.doi.org/10.1103/PhysRevB.57.2493.
[17] A. Groß, Surf. Sci. Rep. 32 (8) (1998) 291.
[18] G.-J. Kroes, Prog. Surf. Sci. 60 (1-4) (1999) 1.
[19] G.-J. Kroes, Science 321 (5890) (2008) 794 (URL http://www.sciencemag.org/content/321/5890/794.abstract).
[20] H.F. Busnengo, A. Salin, W. Dong, J. Chem. Phys. 112 (17) (2000) 7641 (URL http://link.aip.org/link/?JCP/112/7641/1).
[21] P. Gamallo, L. Martin-Gondre, R. Sayós, C. Crespos, P. Larrégaray, Potential energy surfaces for the dynamics of elementary gas–surface processes, in: R. Díez Muiño, H.F. Busnengo (Eds.), Dynamics of Gas–Surface Interactions, Vol. 50 of Springer Series in Surface SciencesSpringer Berlin Heidelberg 2013, p. 25, http://dx.doi.org/10.1007/978-3-642-32955-5_2 (Ch. 2).
[22] A.C. Luntz, J. Harris, Surf. Sci. 258 (1991) 397 (URL http://www.sciencedirect.com/science/article/pii/003960289190934K.).
[23] A. Jansen, H. Burghgraef, Surf. Sci. 344 (1-2) (1995) 149.

[24] M.-N. Carré, B. Jackson, J. Chem. Phys. 108 (9) (1998) 3722.
[25] S. Nave, B. Jackson, J. Chem. Phys. 127 (22) (2007) 224702 (URL http://link.aip.org/link/?JCP/127/224702/1.).
[26] S. Nave, B. Jackson, J. Chem. Phys. 130 (5) (2009) 054701 (URL http://link.aip.org/link/?JCP/130/054701/1.).
[27] B. Jackson, S. Nave, J. Chem. Phys. 135 (11) (2011) 114701 (URL http://scitation.aip.org/content/aip/journal/jcp/135/11/10.1063/1.3634073).
[28] B. Jackson, S. Nave, J. Chem. Phys. 138 (17) (2013) 174705 (URL http://link.aip.org/link/?JCP/138/174705/1).
[29] B. Jiang, R. Liu, J. Li, D. Xie, M. Yang, H. Guo, Chem. Sci. 4 (2013) 3249, http://dx.doi.org/10.1039/C3SC51040A.
[30] J. Harris, J. Simon, A.C. Luntz, C.B. Mullins, C.T. Rettner, Phys. Rev. Lett. 67 (1991) 652, http://dx.doi.org/10.1103/PhysRevLett.67.652.
[31] D.R. Killelea, V.L. Campbell, N.S. Shuman, R.R. Smith, A.L. Utz, J. Phys. Chem. C 113 (48) (2009) 20618.
[32] D.C. Seets, C.T. Reeves, B.A. Ferguson, M.C. Wheeler, C.B. Mullins, J. Chem. Phys. 107 (23) (1997) 10229.
[33] R.A. Olsen, H.F. Busnengo, A. Salin, M.F. Somers, G.J. Kroes, E.J. Baerends, J. Chem. Phys. 116 (9) (2002) 3841.
[34] Y. Xiao, W. Dong, H.F. Busnengo, J. Chem. Phys. 132 (1) (2010) 014704.
[35] Y. Xiao, W. Dong, Phys. Rev. B 83 (2011) 125418, http://dx.doi.org/10.1103/PhysRevB.83.125418.
[36] X.J. Shen, A. Lozano, W. Dong, H.F. Busnengo, X.H. Yan, Phys. Rev. Lett. 112 (2014) 046101, http://dx.doi.org/10.1103/PhysRevLett.112.046101.
[37] A. Groß, A. Dianat, Phys. Rev. Lett. 98 (2007) 206107, http://dx.doi.org/10.1103/PhysRevLett.98.206107.
[38] A. Groß, Chem. Phys. Chem. 11 (7) (2010) 1374, http://dx.doi.org/10.1002/cphc.200900818.
[39] F. Nattino, H. Ueta, H. Chadwick, M.E. van Reijzen, R.D. Beck, B. Jackson, M.C. van Hemert, G.-J. Kroes, J. Phys. Chem. Lett. 5 (8) (2014) 1294.
[40] T. Liang, Y.K. Shin, Y.-T. Cheng, D.E. Yilmaz, K.G. Vishnu, O. Verners, C. Zou, S.R. Phillpot, S.B. Sinnott, A.C. van Duin, Annu. Rev. Mater. Res. 43 (1) (2013) 109, http://dx.doi.org/10.1146/annurev-matsci-071312-121610.
[41] J.H. Rose, J.R. Smith, J. Ferrante, Phys. Rev. B 28 (1983) 1835, http://dx.doi.org/10.1103/PhysRevB.28.1835.
[42] J. Ferrante, J.R. Smith, J.H. Rose, Phys. Rev. Lett. 50 (1983) 1385, http://dx.doi.org/10.1103/PhysRevLett.50.1385.
[43] G.C. Abell, Phys. Rev. B 31 (1985) 6184, http://dx.doi.org/10.1103/PhysRevB.31.6184.
[44] J. Tersoff, Phys. Rev. Lett. 61 (1988) 2879, http://dx.doi.org/10.1103/PhysRevLett.61.2879.
[45] D.W. Brenner, Phys. Rev. B 42 (1990) 9458, http://dx.doi.org/10.1103/PhysRevB.42.9458.
[46] D.W. Brenner, O.A. Shenderova, J.A. Harrison, S.J. Stuart, B. Ni, S.B. Sinnott, J. Phys. Condens. Matter 14 (4) (2002) 783 (URL http://stacks.iop.org/0953-8984/14/i=4/a=312).
[47] A.C.T. van Duin, S. Dasgupta, F. Lorant, W.A. Goddard, J. Phys. Chem. A 105 (41) (2001) 9396, http://dx.doi.org/10.1021/jp004368u.
[48] W.A. Goddard III, B. Merinov, A. van Duin, T. Jacob, M. Blanco, V. Molinero, S. Jang, Y. Jang, Mol. Simul. 32 (3-4) (2006) 251.
[49] J. Ludwig, D.G. Vlachos, A.C.T. van Duin, W.A. Goddard III, J. Phys. Chem. B 110 (9) (2006) 4274, http://dx.doi.org/10.1021/jp0561064.
[50] A.T. Gee, B.E. Hayden, C. Mormiche, T.S. Nunney, J. Chem. Phys. 112 (17) (2000) 7660 (URL http://link.aip.org/link/?JCP/112/7660/1).
[51] P. Valentini, T.E. Schwartzentruber, I. Cozmuta, J. Chem. Phys. 133 (8) (2010) 084703.
[52] A.C. Luntz, D.S. Bethune, J. Chem. Phys. 90 (2) (1989) 1274 (URL http://link.aip.org/link/?JCP/90/1274/1).
[53] G. Kresse, J. Furthmüller, Comput. Mater. Sci. 6 (1) (1996) 15 (URL http://www.sciencedirect.com/science/article/pii/0927025696000080).
[54] G. Kresse, J. Furthmüller, Phys. Rev. B 54 (1996) 11169, http://dx.doi.org/10.1103/PhysRevB.54.11169.
[55] J.P. Perdew, K. Burke, M. Ernzerhof, Phys. Rev. Lett. 77 (1996) 3865, http://dx.doi.org/10.1103/PhysRevLett.77.3865.
[56] P.E. Blöchl, Phys. Rev. B 50 (1994) 17953, http://dx.doi.org/10.1103/PhysRevB.50.17953.
[57] H.J. Monkhorst, J.D. Pack, Phys. Rev. B 13 (1976) 5188, http://dx.doi.org/10.1103/PhysRevB.13.5188.
[58] M. Methfessel, A.T. Paxton, Phys. Rev. B 40 (1989) 3616, http://dx.doi.org/10.1103/PhysRevB.40.3616.
[59] R.A. Olafson, M.A. Thomas, H.L. Welsh, Can. J. Phys. 39 (3) (1961) 419, http://dx.doi.org/10.1139/p61-042.
[60] G. Mills, H. Jónsson, Phys. Rev. Lett. 72 (1994) 1124.
[61] G. Mills, H. Jónsson, G.K. Schenter, Surf. Sci. 324 (2-3) (1995) 305.
[62] H. Jónsson, G. Mills, K.W. Jacobsen, Classical and Quantum Dynamics in Condensed Phase Simulations, in: B.J. Berne, G. Ciccotti, D.F. Coker (Eds.), World Scientific, Singapore, 1998.
[63] S.S.M. Wong, Computational Methods in Physics and Engineering, World Scientific, Singapore, 1997.
[64] M.A. Collins, Theor. Chem. Accounts 108 (2002) 313, http://dx.doi.org/10.1007/s00214-002-0383-5.
[65] X.G. Wang, E.L. Sibert III, J. Chem. Phys. 111 (10) (1999) 4510 (URL http://link.aip.org/link/?JCP/111/4510/1).
[66] A. Lozano, X.J. Shen, W. Dong, H.F. Busnengo, X.H. Yan, Accurate Reaction Specific Force Fields for Methane Dissociation on Metal Surfaces, 2015. (in preparation).
[67] T.D. Sewell, D.L. Thompson, Int. J. Mod. Phys. B 11 (09) (1997) 1067, http://dx.doi.org/10.1142/S0217979297000551.
[68] B. Jackson, The effects of lattice motion on gas–surface reactions, in: R. Díez Muiño, H.F. Busnengo (Eds.), Dynamics of Gas–Surface Interactions, Vol. 50 of Springer Series in Surface SciencesSpringer Berlin Heidelberg 2013, p. 213, http://dx.doi.org/10.1007/978-3-642-32955-5_9 (Ch. 9.).
[69] L. Chen, H. Ueta, R. Bisson, R.D. Beck, Rev. Sci. Instrum. 84 (5) (2013) 053902 (URL http://link.aip.org/link/?RSI/84/053902/1).
[70] G.R. Schoofs, C.R. Arumainayagam, M.C. McMaster, R.J. Madix, Surf. Sci. 215 (1989) 1.
[71] M. Mastromatteo, B. Jackson, J. Chem. Phys. 139 (19) (2013) (URL http://scitation.aip.org/content/aip/journal/jcp/139/19/10.1063/1.4829678).
[72] J. Higgins, A. Conjusteau, G. Scoles, S.L. Bernasek, J. Chem. Phys. 114 (12) (2001) 5277, http://dx.doi.org/10.1063/1.1349895.
[73] R. Bisson, M. Sacchi, T. Dang, B. Yoder, P. Maroni, R. Beck, J. Phys. Chem. A 111 (49) (2007) 12679.
[74] D.J. Oakes, M.R.S. McCoustra, M.A. Chesters, Faraday Discuss. 96 (1993) 325.
[75] A.K. Tiwari, S. Nave, B. Jackson, Phys. Rev. Lett. 103 (2009) 253201, http://dx.doi.org/10.1103/PhysRevLett.103.253201.
[76] S. Nave, B. Jackson, Phys. Rev. Lett. 98 (2007) 173003, http://dx.doi.org/10.1103/PhysRevLett.98.173003.
[77] H.F. Winters, J. Chem. Phys. 64 (9) (1976) 3495.
[78] L.B.F. Juurlink, R.R. Smith, D.R. Killelea, A.L. Utz, Phys. Rev. Lett. 94 (2005) 208303, http://dx.doi.org/10.1103/PhysRevLett.94.208303.
[79] R. Beck, A. Utz, Quantum-state resolved gas/surface reaction dynamics experiments, in: R. Díez Muiño, H.F. Busnengo (Eds.), Dynamics of Gas–Surface Interactions, Vol. 50 of Springer Series in Surface SciencesSpringer Berlin Heidelberg 2013, p. 179, http://dx.doi.org/10.1007/978-3-642-32955-5_8 (Ch. 8).
[80] G.A. Somorjai, Introduction to Surface Chemistry and Catalysis, 2nd edition John Wiley & Sons, New York, 1994.
[81] M.J. Bronikowski, W.R. Simpson, B. Girard, R.N. Zare, J. Chem. Phys. 95 (11) (1991) 8647 (URL http://link.aip.org/link/?JCP/95/8647/1).
[82] M.J. Bronikowski, W.R. Simpson, R.N. Zare, J. Phys. Chem. 97 (10) (1993) 2194, http://dx.doi.org/10.1021/j100112a021.